Chapter

Realization of the Quantum Confinement

Eugen M. Sheregii

Abstract

In this chapter the three main technologies are described, which allows for the implementation of quantum structures (QS)—quantum wells (QWs) and hetero-structures. These are liquid phase epitaxy (LPE), molecular beam epitaxy (MBE), and metal-organic chemical vapor deposition (MOCVD). The most important properties, including the quantum Hall effect (QHE), of two-dimensional electron gas (2DEG) arising in a heterojunction on the boundary of two phases—the so-called interface—are also presented. The 2DEG properties in different kinds of QW are described. Double quantum wells as interesting example of quantum structure is considered also including such a spectacular quantum-mechanical phenomenon as splitting into symmetrical and anti-symmetrical states.

Keywords: hetero-structure, liquid phase epitaxy, molecular beam epitaxy, interface, single quantum well, quantum well, electron transport in quantum structures, two-dimensional electron gas (2DEG), quantum Hall effect, Shubnikov-de Haas effect, high electron mobility transistors

1. Introduction

The entrapping of electrons in an infinite quantum well (QW) is one of the basic issues of quantum mechanics showing its difference from classical mechanics. In fact, nature has given us a natural quantum well—atom. Coulomb's potential of the atomic nucleus creates the edges of this well (see **Figure 1**)—a very narrow well, about 1 Å (10^{-10} m) width. As it was shown in previous chapters, in such a narrow well the electron can occupy only certain energy states—discrete and not continuous energy values—as it is in the macro-world. This was indicated by the linear emission spectra of atoms discovered at the end of the nineteenth century. Their interpretation forced Niels Bohr to introduce discrete electronic states, so alien to classical physics, into the historically first quantum atom theory, which is familiar from the course of high school physics.

However, this rectangular quantum well, which is the subject of students' exercises in quantum mechanics course, until the early 1980s was a theoretical issue. As will be shown in the next paragraphs, the progress of semiconductor technology, particularly the development of the *molecular beam epitaxy* (MBE), allowed the production of hetero-structures with *very sharp interface* (transition between two material phases) and later also quantum wells with width less than 100 angstroms and with finite potential edges, which changed the situation cardinally: the issue of two-dimensional electron gas (2DEG) appeared and the quantum Hall effect (QHE)

IntechOpen

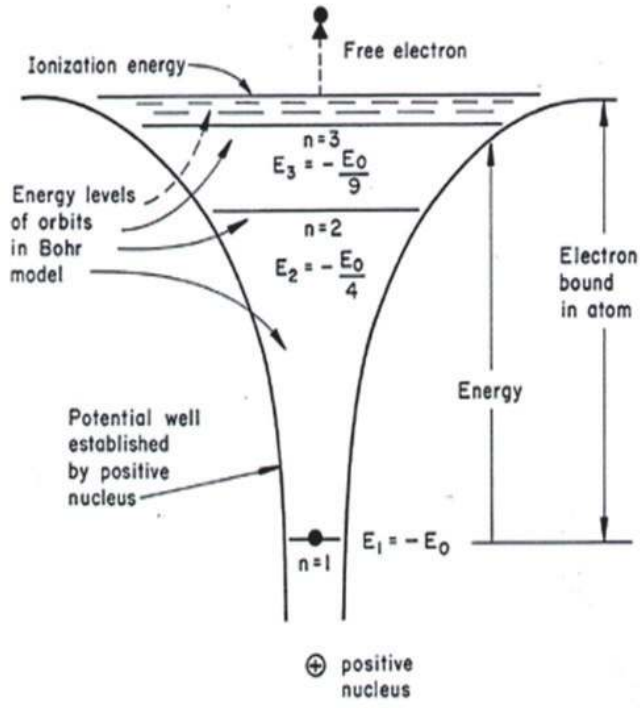

Figure 1.
Natural quantum well of the hydrogen atom created by the potential of the atomic nucleus $E = -e/r$.

was discovered—a qualitatively new phenomenon. In this manner, quantum wells are soluble models and have provided tests for quantum theory. Also, the applications appeared very quickly—already in the 80-ch formed hetero-lasers—the first solid-state lasers, and transistors on hetero-structures sizes that do not exceed of 100 nm, which led to the production of modern micro-processors with a packing density of 20,000 transistors in a spatial centimeter.

In this way quantum mechanics contributed to the emergence of the third industrial revolution—electronics and radio-communications—as well as the promised fourth one, computerization (without microprocessors would be impossible) and global communication network, the Internet, which without semiconductor lasers would not have been created either. To achieve this duty, it was necessary to develop appropriate technologies. The first was *liquid phase epitaxy* (LPE).

2. LPE technology and the hetero-structure production

LPE is the deposition from a liquid phase (a solution or melt) of a thin monocrystalline layer which is isostructural to the crystal of the substrate [1]. For the production of hetero-structures, the LPE was first used by Zhores Alferov with colleagues at the Ioffe Physical and Technical Institute in St. Petersburg [2]. They produced the hetero-structures based on the GaAs/AlGaAs n-p heterojunctions (unlike the usual p-n junction, which can be called a homo-junction) [3]. The zone scheme of such p-n heterojunction is presented in **Figure 2**. This diagram clearly shows that a quantum well forms at the interface in the conduction band from the side of GaAs, i.e., a semiconductor with a smaller energy gap (about 1.4 eV). In the case of the solid solution $Al_{0.3}Ga_{0.7}As$ that is 1.9 eV, QW is created by the discontinuity in the conduction band profile as a function of distance *x*. The discontinuity takes place in the case of the valence band too, and it manifests itself as a leap called

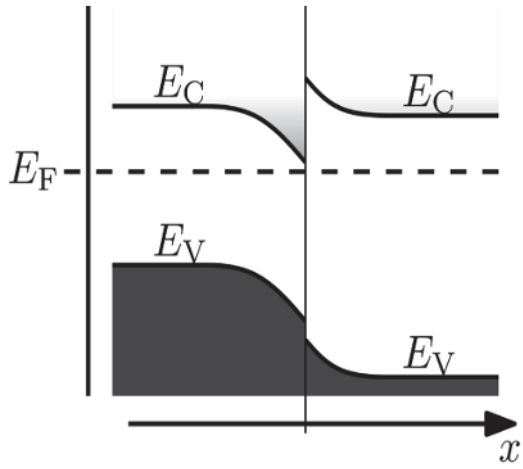

Figure 2.
Energy band diagram for the GaAs/AlGaAs heterojunction point QW, which would mean that the well is filled with electrons.

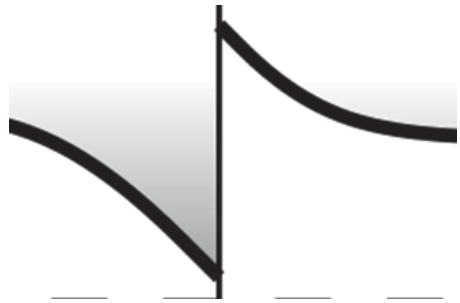

Figure 3.
Triangular QW formed in the conduction band at the heterojunction GaAs/AlGaAs shown in ***Figure 2****.*

offset. The QW exists only for electrons, and if the electron concentration increases, the Fermi level (FL) moves upwardly, and the conduction band will intersect at the QW, shown enlarged separately in **Figure 3**. You can see that it is a QW with a triangular shape. It should be noted that the shape of QW takes place also in the metal-oxide semiconductor (MOS) structures. Energy states for electrons in the real QW for the $Al_{0.3}Ga_{0.7}As$/GaAs junction were calculated by Zawadzki and Pfeffer [4]: the well depth is about 500 meV, and the resonance states occur at 200 meV and 360 meV from the bottom of the well. According to these calculations, the width of the well is about 200 Å or 0.02 μm. This fact explains why heterostructures with QW visible in the experiment could not have been obtained earlier using known crystal growth technologies and obtaining the p-n junctions by diffusion method. These methods did not allow for such a required change in the composition over several crystal lattice parameters. LPE methods have the advantage that with relative simplicity, a liquid AlGaAs solution with the necessary composition is poured onto a previously prepared (well-polished and heated to a temperature of about 600°C) GaAs substrate and the substrate will not melt during crystallization. Also, the diffusion of atoms is too slow for them to penetrate into the solid phase. Thanks to this, the required sharpness of the transition (junction) is preserved. However, the thickness of the AlGaAs layer should not exceed 1–2 μm. The last limitation is related to the upper layer stresses, resulting from incompatibility of the crystal lattice parameters of the substrate and the applied layer—so-called the lattice mismatch—minimal in the case of the GaAs and the AlGaAs solid

solution with 30% AlAs as it is only 0.01 Å (4.65 Å for GaAs and 4.66 Å for $Al_{0.3}Ga_{0.7}As$) [4]. The first semiconductor lasers were produced thanks to LPE technology developed for the GaAs/AlGaAs heterojunction in the early 1970s [3]. However, more advanced technology was needed to improve the production of the heterojunction lasers.

3. MBE technology and the production of the solid-state QW

3.1 Description of the MBE technology

The width of the quantum well in the case of GaAs/$Al_{0.3}Ga_{0.7}As$ heterojunction is on the order of 150–200 Å, and the technology capabilities of LPE technology are on the border of these requirements to keep the production of devices based on them. For this reason, in the 1970s, a fundamentally new technology was developed that allowed a significant leap in the development of the semiconductor devices as well as the solid-state physics, generally. The MBE technology is based on the method of the crystal growth from the gas phase, but the use of computers made it possible to achieve precision previously unattainable [5]. First of all, it concerns the composition control (the composition control is so closely that practically every atom deposited on the substrate is calculated) but it is also the substrate temperature is much lower (450°C) than in the LPE method what is important because it reduces the diffusion intensity of atoms and has significantly improved the quality of the interface. But on the other hand, it is an expensive technology because it requires a high vacuum—10^{-11} Torr—which must be sustained continuously over several years. On the other hand, this extraordinary high vacuum allows the use of mass spectroscopy in the reactor for precise control of the composition and existing impurities. It should be recalled that the intrinsic properties of semiconductor materials were achieved only after chemists learned to clean the input materials from impurities at a concentration level of 10^{-12} cm^{-3}, which in turn means chemical purity 99.9999999%. Achieving such chemical purity of input materials requires huge amounts of labor and energy. The use of a high vacuum of the order of 10^{-11} Torr means additional "dilution" in the dopant concentration in reactor, which allowed the use of input materials in the effusors—sources of elements in the MBE machine—with a chemical purity lower by one row: 99,999999%.

The MBE process was noticed in the late 1970s at Bell Telephone Laboratories by Arthur and LePore [6]. But, the main role of this method has become the production of quantum structures (QS) from the 1980s [7] and above all—heterostructures and quantum wells.

Another technology that also relates to high tech is the metal-organic chemical vapor deposition (MOCVD) in some ways competitive to MBE because it allows obtaining high-quality quantum structures also.

3.2 MOCVD technology

The MOCVD involves the use of gases—carriers of elements used in QS built from GaAs, AlGaAs, InGaAs, and others. We call these gases metal-organic, for example, three-methyl-gal ($Ga(CH_3)_3$), three-methyl-aluminum ($Al(CH_3)_3$), or three-hydrogen of arsenic (AsH_3). These substances are contained in bottles in a liquid state at about – 60°C, and are admitted as gases (still cool) to a reactor where the touching surface of the substrate at 500°C to immediately distributed to the constituent elements and relatively heavy metals as Al, As, Ga deposited on the substrate surface at this time how much lighter C and H are pumped out of the

reactor. MOCVD technology is much cheaper to operate (no vacuum) and is used as industrial manufacturing technology for QS and devices on their base.

3.3 Two-dimensional electron gas (2DEG)

The improved interface quality of hetero-structures through the use of MBE technology has led to the discovery of the unique properties of two-dimensional electron gas. The point is that the quantum well, which is located at the interface in the conduction band, naturally fills with electrons. The electrons are located in a layer with a thickness less than 200 Å. This means that they are actually in a plane that adheres to the interface (parallel to the interface) with a negligible thickness compared to two other dimensions. That is, a two-dimensional electron gas is created at the interface, which we will denote as 2DEG.

One of the basic properties of 2DEG is that electrons occupy one of the energy states of the quantum well at the interface. We will call this state as the energy sub-band and the dispersion law—energy dependence from quasi-momentum $\mathcal{E}(k)$ for 2DEG can be written in the case where the interface plane is the plane (yz) and x—the direction of growth of the hetero-structure layers (as it is shown in **Figure 2**), in the following way:

$$E(k) = E_i + \hbar^2 \frac{k_z^2 + k_y^2}{2m^*} \tag{1}$$

where i is 1, 2, 3, ... number of the sub-band, $\hbar = h/2\pi$ the Planck constant, and $\mathcal{E}_i$ is the energy value of the sub-band i, m^* effective mass of electrons.

It is obvious that the dispersion law (1) is a consequence of the restriction of movement in the x direction, in other words, by the quantum confinement, which causes the energy quantization.

Graphically the expression (1) is presented in **Figure 4**. The parabolic sub-band corresponds to each value of i.

The density of states function shown in **Figure 5** corresponds to such a law of dispersion. In contrast to the bulk material where the function of density of states is proportional to $\sqrt{E}$, in the 2D case we have steps corresponding to each value of E_i: $D(E) = i\frac{m^*}{\pi\hbar^2}$, where m^* is the effective mass of electrons.

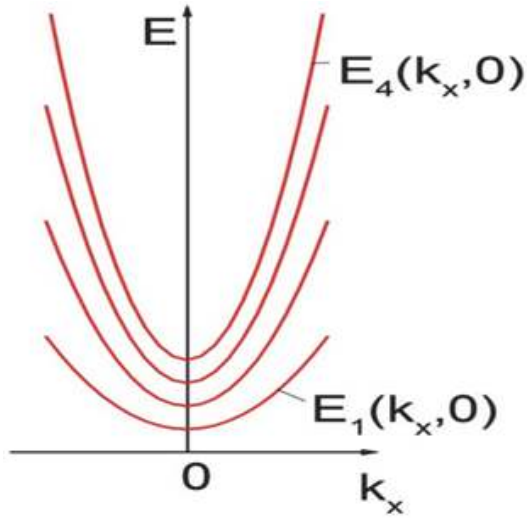

Figure 4.
The energy sub-bands corresponding to Eq. (1) where $k_y = 0$.

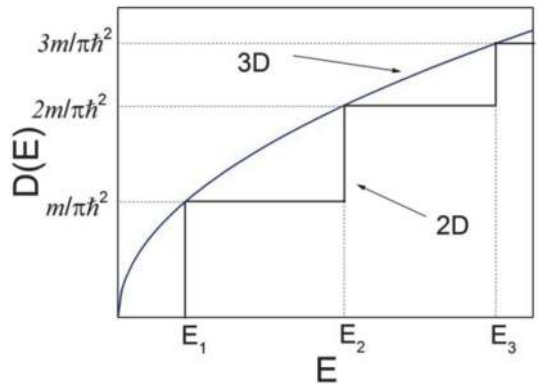

Figure 5.
The function of the state density for 2DEG in a quantum well.

This stepped nature of the function of the state density for 2DEG in a quantum well is manifested in a multitude of phenomena including the dependence of the current through the heterojunction on the gate voltage, on which the transistor operated on the GaAs/AlGaAs hetero-structure is based, the so-called high electron mobility transistor (HEMT) [8].

3.4 Quantum Hall effect

The most spectacular expression of 2DEG in QS is quantum Hall effect discovered by von Klitzing [9] in 1980. We can say that QHE is a manifestation of quantum mechanics on macroscopic scales [10].

Experimentally, QHE shows the remarkable transport data as it is shown in **Figure 6** for a real device in the quantum Hall regime which is the same as in classical Hall effect when magnetic field ***B*** is perpendicular to the plane of the sample *xy* and to the current *I* directed along the *x*-axis. Then, in the direction perpendicular to the movement of the charges (electrons), an additional transverse voltage is created, called the Hall voltage U_H. In classical Hall effect, the Hall resistance R_H is simply a linear function of magnetic field and resistivity also $\rho_{xy} \sim B$. In QHE we see a series of the so-called Hall plateaus in which ρ_{xy} is a universal constant

$$\rho_{xy} = \frac{1}{\nu}\frac{h}{e^2} \tag{2}$$

(where e is the electron charge and $\nu = 1,2,\ldots$ an integer which means the number of the states occupied by electrons under the Fermi level and is called as *filling factor*) independent of all microscopic details (including the precise value of the magnetic field). Associated with each of these plateaus is a dramatic decrease in the dissipative resistivity $\rho_{xx} \rightarrow 0$ which drops as much as 13 orders of magnitude in the plateau regions.

QHE is a two-dimensional phenomenon because when the magnetic field B is perpendicular to the plane of the hetero-structure, the movement of the electrons in the plane of the quantum well is completely quantized. This quantization is universal and independent of all microscopic details such as the type of semiconductor material, the purity of the sample, the precise value of the magnetic field, and so forth. The growth of the magnetic field causes an increase of the distance between Landau levels, $\hbar\omega_c = eB/m^*$, and when the Fermi level is located between Landau levels then, for the electrons occupying the Fermi level, there are no states to

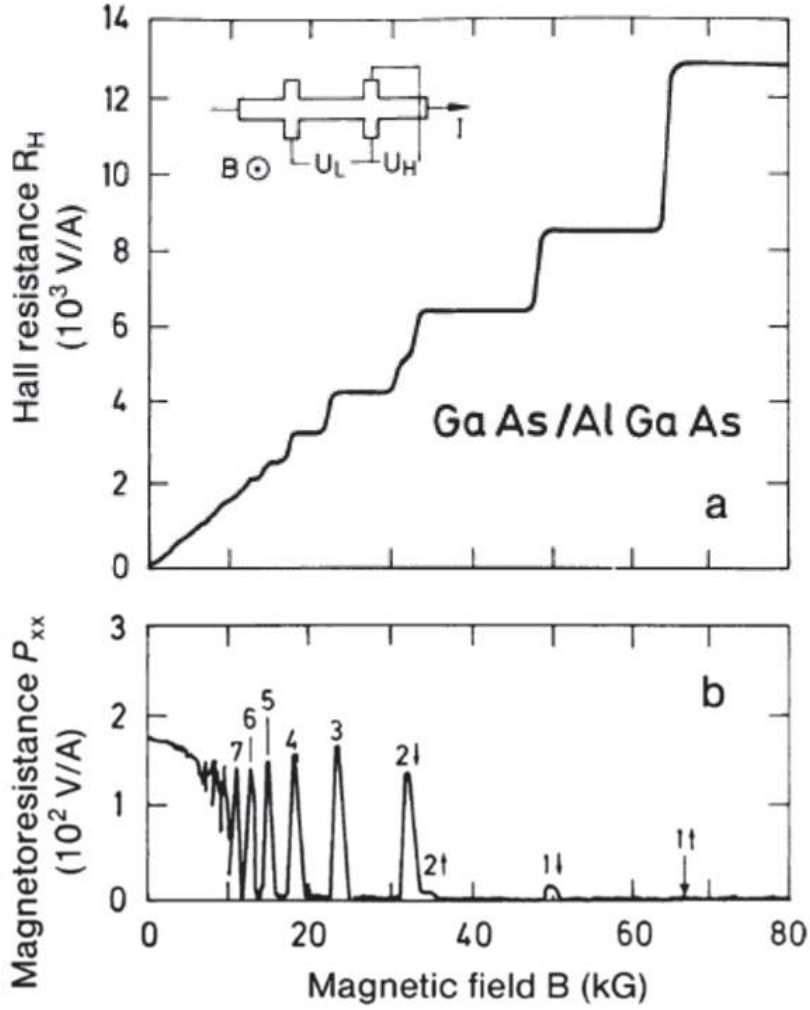

Figure 6.
(a) QHE (the Hall resistance R_H *as function of magnetic field* B*); (b) the Shubnikov-de Haas oscillations (magnetoresistance* ρ_{xx}(B)*) for hetero-structure GaAs/AlGaAs [11].*

dissipate, and it cannot move in the electric field—no electric current exists and ρ_{xx} is zero. In this situation the Hall voltage is constant until the Fermi level does not reach the next Landau level, and the next step of the Hall voltage takes place (in the case of bulk material, there are always scattering channels causing the presence of electric current in a strong magnetic field, therefore the dependence of the Hall voltage on the magnetic field is continuous and reflects the continuity of the density function of states (see **Figure 5**)).

As a result, the QHE is now used to maintain the standard of electrical resistance by metrology laboratories globally.

The magnitude h/e^2 = 25,812,80 Ω is so important as constant of the fine structure in the quantum electrodynamics.

3.5 Quasi-rectangular quantum well

To obtain a quantum well with a rectangular shape, it should be placed close enough to two heterojunctions as shown in **Figure 7**. How close? The experiment shows that at a 200 nm distance, two GaAs/AlGaAs heterojunctions exhibit the properties of a rectangular QW [11]. It can be seen from **Figure 7** that these two

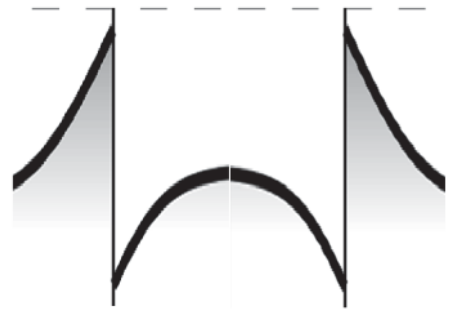

Figure 7.
QW formed from two heterojunctions.

heterojunctions must be a mirror image of each other: first is the growth of the GaAs layer—the QW—and next is of the AlGaAs layer, the *barrier* for QW. It is clear that such a well has a form still far from a rectangular well, but it is already known how to achieve the form of a rectangular potential: stretch the middle GaAs layer as much as possible. In this case we would have a very wide quantum well.

But there is another way of special engineering allowing to obtain a real rectangular QW considered in Section 3.7. Modeling of quasi-rectangular QW using heterojunctions InGaAs/InAlGaAs will be shown in the next paragraph.

3.6 Modeling of quasi-rectangular QW based on the InGaAs/InAlGaAs heterojunctions

Heterojunctions InGaAs/InAlGaAs are important advantage in comparison with GaAs/AlGaAs because low effective mass of electrons—adding the InAs to the QW material, i.e., to GaAs—allows effective mass to be significantly reduced from 0.65 m_0 for GaAs to even $0.4m_0$ for InGaAs with 65% of the InAs. This means that the electron mobility is almost doubled, which is the main goal of the HEMT modeling. On the other hand, the composition of two solid solutions—$In_xGa_{1-x}As$ for QW and $In_yAl_{1-y}As$ for a barrier—can be selected so as to minimize mismatch of the lattice parameters. Such hetero-structures are isomorphic. In this way, the issue was the production of QW for HEMT based on isomorphic hetero-structures. That could be used in industry, so the production technology also had to be industrial. To implement this duty, the MOCVD technology was developed at the Institute of Electronic Materials Technology (ITME) in Warsaw for the production of isomorphic hetero-structures based on InGaAs/InAlAs heterojunctions. The structures are consisted from single $In_xGa_{1-x}As$ QW and from the two $In_yAl_{1-y}As$ layers—barriers. Four types (see **Table 1**) of different forms of structures with a single QW (SQW) were produced by MOCVD on semi-insulating GaAs at ITME by W. Strupiński group and tested at the Center for Microelectronics and Nanotechnology at the University of Rzeszów during the years 2005–2014 [12, 13]. After that, the program of producing double quantum wells (DQW) and multiple quantum wells (MQW) was developed in years 2015–2018 [14–16].

3.6.1 SQWs

In **Figure 8**, cross section of SQWs obtained by MOCVD on semi-insulated GaAs substrates is shown. If the δ-doping layer with Si is at the top above QW and below at QW then, the shape of the QW is symmetrical as in **Figure 9**, if and only at the top, a QW is asymmetric as in **Figure 10**.

Sample	Channel parameters			δ-doping donor concentration (10^{12} cm^{-2})
	Composition of In (%)	Thickness (nm)	QW profile	
1093	75	20	Sharp interface	2.5
1098	65	20	Changing composition in a channel	5.0
1607	65	23.5	Sharp interface	3.5
1088	53	20	Sharp interface	0.7

Table 1.
Parameters of the channels and descriptions of the interfaces for the SQWs.

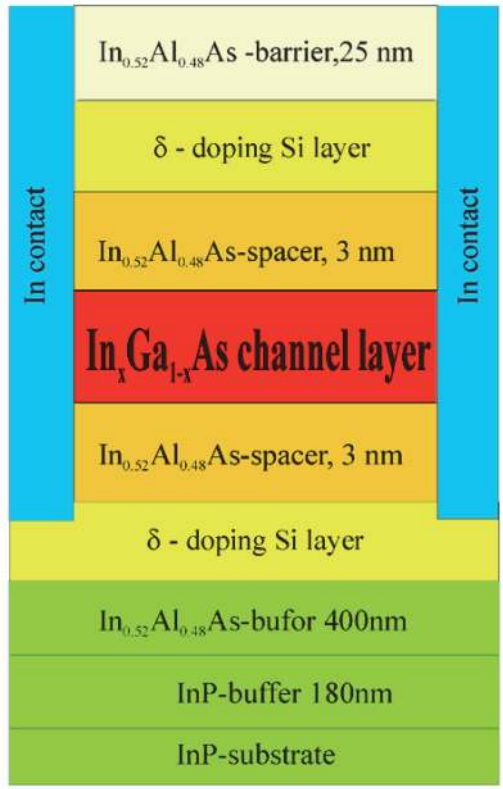

Figure 8.
The cross section of the SQW grown by the MOCVD.

The magneto-transport measurements, i.e., Hall's resistance curves R_H (B) or R_{xy} (B) and longitudinal magnetoresistance ρ_{xx} (B), were performed for all the presented SQWs. It is clearly seen in **Figure 9** the plateau on the curve R_{xy} (B) corresponding to the filling factors ν = 3, 6, 8, etc. Explanation of this values of filling factor is presented in **Figure 10** where the curve of R_{xy} (B) as well as R_{xx} (B) is interpreted.

In order to interpret the curves R_{xy} (B) and R_{xx} (B) for the QW 1088 which is practically a triangle QW (the electrons are located in the bottom left triangle), the theory developed by W. Zawadzki [17] was used

$$(a+b)a^{1/2}b^{1/2} + (b-a)^2 \ln\left|\frac{b^{1/2}-a^{1/2}}{(b-a)^{1/2}}\right| = \left[\frac{E_g^*}{2m_c^*}\right]^{1/2} \times 4eF\hbar\pi(i+3/4) \qquad (3)$$

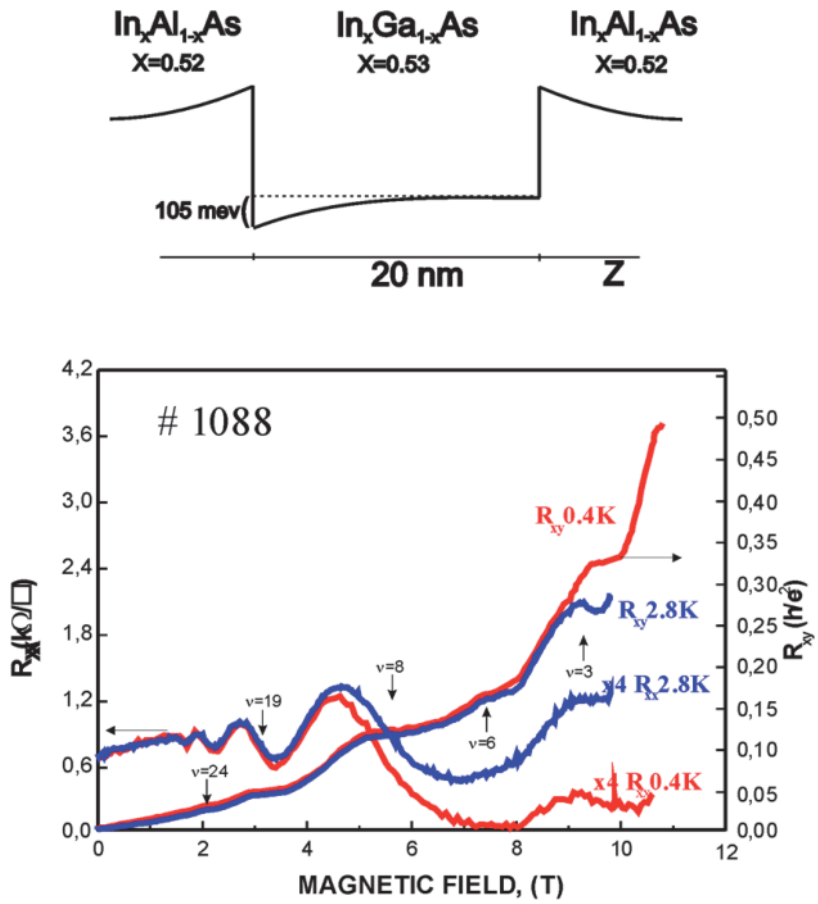

Figure 9.
*The Hall resistivity curve R_{xy} (B) and longitudinal magnetoresistivity curve R_{xx} (B) for the SQW 1088 (see **Table 1**) with asymmetric shape of QW [12, 13].*

where $a = E - E_{\perp}$; $b = E_g + E + E_{\perp}$; E is the energy of sub-band in QW, $E_{\perp}$ is the Landau level energy sought, E_g is the energy gap, and F is the electrical field strength caused by interface and is determined by linear potential $U = eFz$.

Results of calculations presented in **Figure 10** show that the intersection of Landau levels of two energy sub-subbands takes place; hence the picture of QHE and SdH oscillations is more complicated but is perfectly explained by the theory for the triangle QW.

3.7 Special engineering of a rectangular QW

The special engineering of QW involves changing the composition of the solid solution in the well to compensate for the reduction in potential at the left and right corner of the bottom of the well. The schema of such compensation is shown in **Figure 11**: there is a change in the composition in the quantum well from the left side of the interface and the right side too. This mild change from x = 0.53 to 0.65 (on the left and vice versa from 0.65 to 0.53 on the right) accurately compensates for the value of the energy gap, as well as the decrease in the bottom of the well—the conduction band—so that it becomes almost flat.

This fact that we are dealing with an excellent rectangular quantum well confirms the experimental magneto-transport curves obtained for QW 1098.

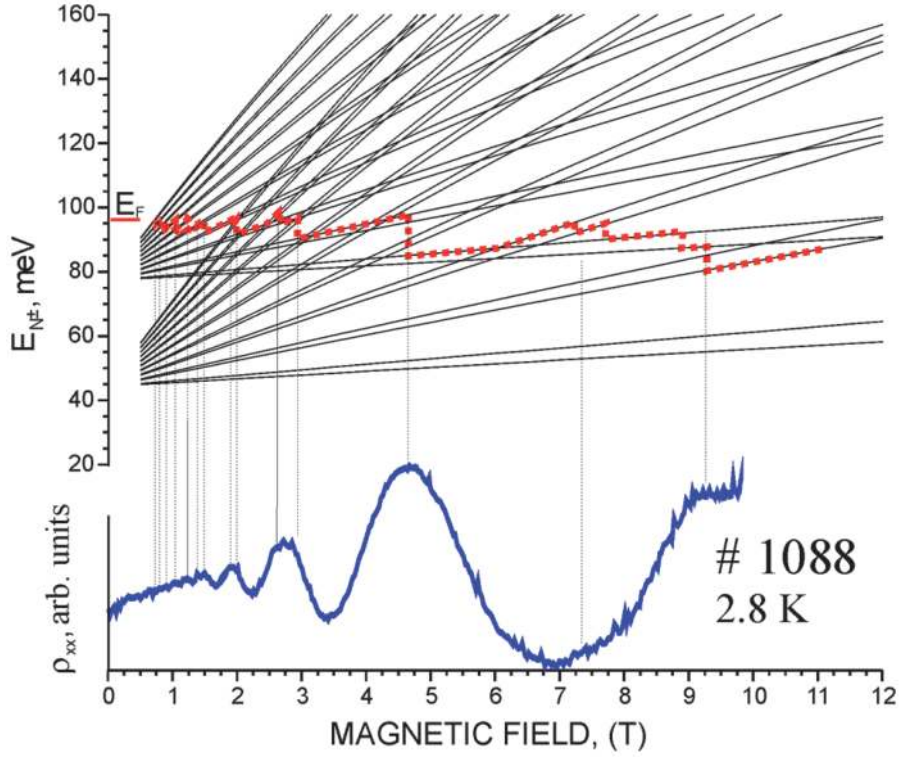

Figure 10.
Interpretation of the QHE curve and magnetoresistance curve for three-angle SQW 1088 [12, 13].

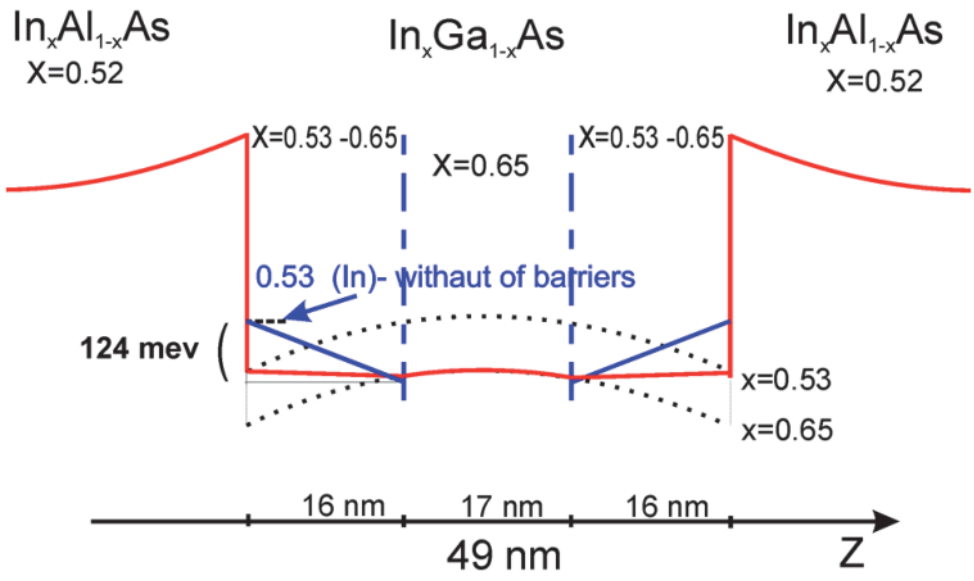

Figure 11.
Schema of the rectangular QW (1098) engineering [13].

The theoretical interpretation of experimental curves presented in **Figure 12** was performed by curves of the Landau level (LL) (presented above) calculated according the theory of Zawadzki [17]:

$$\frac{(E-E_\perp)(E_g+E+E_\perp)}{E_g}=\frac{\hbar^2\pi^2(i+1)^2}{2m_0^* a^2 k} \tag{4}$$

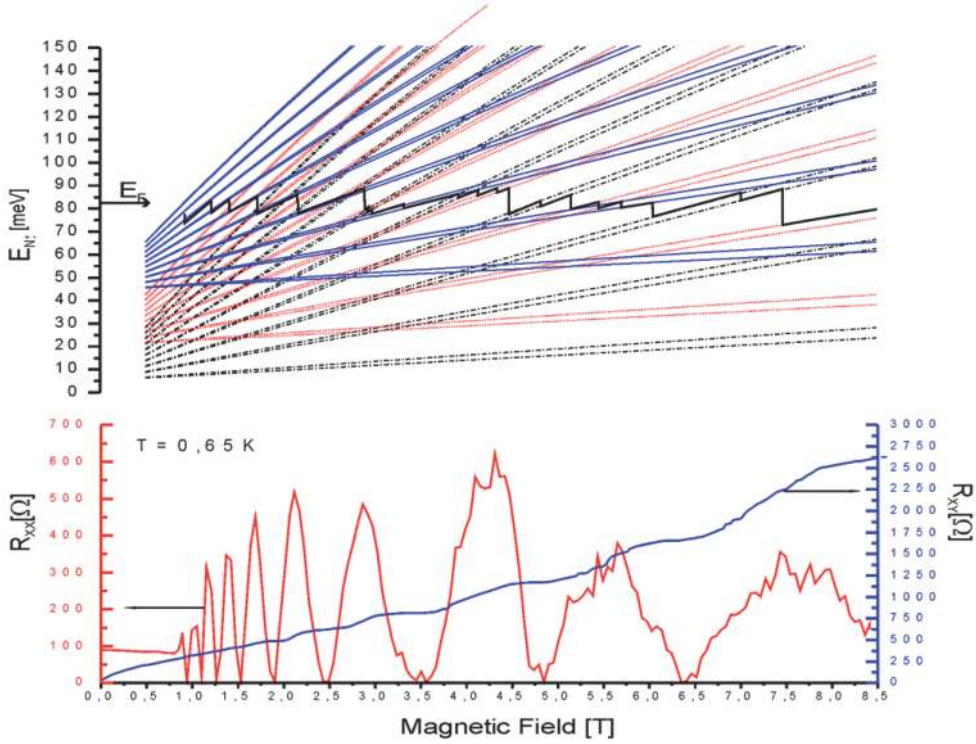

Figure 12.
The Hall resistivity curve R_{xy} (B) and longitudinal magnetoresistivity curve R_{xx} (B) for the SQW 1098 [13].

$$E_{\perp} = -\frac{E_g}{2} + \frac{E_g}{2}\sqrt{1 + \frac{4\mu_B B}{E_g}\left[f_1 \frac{m_0}{m_c^*}\left(n + \frac{1}{2}\right) \pm \frac{1}{2} g_0^* f_2\right]} \tag{5}$$

$$f_1 = \frac{\left(E_g + \Delta\right)\left(E_{\perp} + E_g \tfrac{2}{3}\Delta\right)}{\left(E_g + \tfrac{2}{3}\Delta\right)\left(E_{\perp} + E_g + \Delta\right)} f_2 = \frac{E_g + \tfrac{2}{3}\Delta}{E_{\perp} + E_g + \Delta} \tag{6}$$

where E is the energy of sub-band in QW, $E_{\perp}$ is the Landau level energy sought, and E_g is the energy gap, while Δ is the value of the spin-orbit splitting, i is the number of sub-band, n is the number of LL, μ_B is the Bohr magneton, and m_c^* is the effective mass of electrons on the bottom of the conduction band. As you can see in the right side of Eq. (4), the energies of states in a rectangular well with a correction for the finite potential through coefficient k are described.

It is seen that theoretical curve of the Fermi level in the course of the magnetic field reflected both the plateau of the R_{xr}(B) and the maxima of the R_{xx}(B) experimental curves: the QHE plateau positions correspond to the FL positions between LL that simultaneously correspond to the minima of the SdH oscillations.

In this way, it can be said that thanks to special engineering, it has been possible to make a *real rectangular potential of QW described by quantum-mechanical theory*.

3.8 Double quantum well

3.8.1 The SAS-splitting

Technology successes have allowed us to experimentally confirm one interesting quantum-mechanical phenomenon—it concerns the splitting into symmetrical and anti-symmetrical states thanks to the *Pauli exclusion principle*, in other words, *exchange interaction*.

Pauli's principle was known in relation to atoms, molecules, and crystal theory, while for the first time an artificial object was generated in which this principle was spectacularly confirmed—in an electron system consisting of two closely spaced QWs. In the inset of **Figure 13**, the potential profile of two QWs with narrow barrier between wells is shown. Due to narrow barrier, the tunneling among QWs is facilitated and electrons in these two QWs constitute the common electron system. This system is subject to Pauli's principle, as a result of which there are electron states in which the spin part of the wave function has the opposite sign—symmetrical and anti-symmetrical functions and correspondently symmetrical and anti-symmetrical states—separated by the energy gap, the so-called SAS gap.

3.8.2 Magneto-transport phenomena

For first time, this effect was considered in the work of G. S. Boebinger et al. [18] where the GaAs/AlGaAs DQWs produced by MBE technology were investigated. This fact was observed experimentally on the QHE curves: where quantum Hall states at odd integer ν (filling factor) were missing, the ν = odd quantum Hall states originate from the SAS gap [18].

Magneto-transport phenomena were studied also for the InGaAs/InAlAs DQWs. In addition to QHE and SdH oscillation, magneto-phonon resonance was also studied and interpreted using the LL energy theory for the DQW [19]:

$$E_{nj} = \left(n - \frac{1}{2}\right)\hbar\omega_{cj} + E_j + V_{nj}^F \tag{7}$$

$$V_{nj}^F = -\frac{1}{2\pi}\sum_{n'j'}\int_0^{+\infty} dq_{xy}q_{xy} \times \left\{\frac{1}{\exp\left\{\left[E_{n'j'} - \mu_c\right]/k_BT\right\} + 1}\right\} \times \left|A_{n'n}\left(q_{xy}\right)\right|^2 V_{jj'}^F\left(q_{xy}\right) \tag{8}$$

where j is number of the energy sub-band, n is number of the LL, $\left|A_{n'n}\left(q_{xy}\right)\right|^2$ is matrix element for two Landau levels n and n', $V_{jj'}^F\left(q_{xy}\right)$ is factor of screening [19].

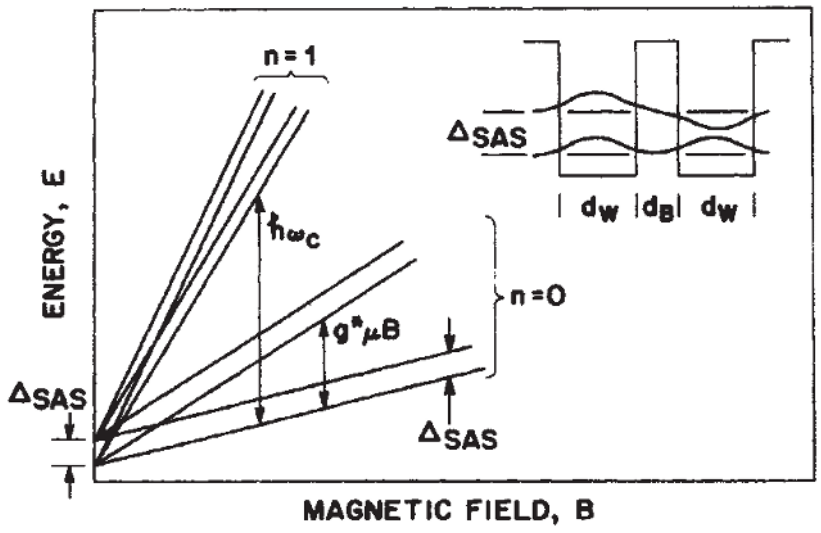

Figure 13.
Three kinds of splitting of energy states in DQW: cyclotron $\hbar\omega_c$, spin splitting $g^*\mu_B B$, and Δ_{SAS}—splitting on the symmetric and antisymmetric states.

The combination of this DQW theory with the Landau level theory presented above for SQW (Eq. (4)) gives us the following equation:

$$\frac{(E - E_\perp)(E_g + E + E_\perp)}{E_g} = \frac{\hbar^2\pi^2(i+1)^2}{2m_0^* a^2 k} \pm (\Delta_0 + 0.38E_\perp) \tag{9}$$

Adding Eqs. (5) and (6) to this (9) allows the calculation of the LL energy in DQW. The value of Δ_{SAS} in Eq. (9) depends from magnetic field B as function of energy $E_\perp$:

$$\Delta_{SAS} = \Delta_0 + 0.38\ E_\perp. \tag{10}$$

where Δ_0 is the Δ_{SAS} value without magnetic field.

In **Figure 14**, the LL energies for DQW 2506 (see **Table 1**) and interpretation of the R_{xy} curve obtained for this DQW are presented. The splits caused by the SAS gap are clearly seen on the R_{xx} (B) curve. These are experimental data that indirectly indicate the SAS-splitting in DQW. But on the same DQW it was possible to make optical measurements from which the energy states were directly determined.

These optical measurements that concern the optical reflection in the infrared region were made using infrared microscope.

3.8.3 Direct determination of the energy states in the DQW

The experiment on the infrared reflection was performed at the Frascati National Laboratory in Italy. Synchrotron radiation served the brilliant infrared radiation source.

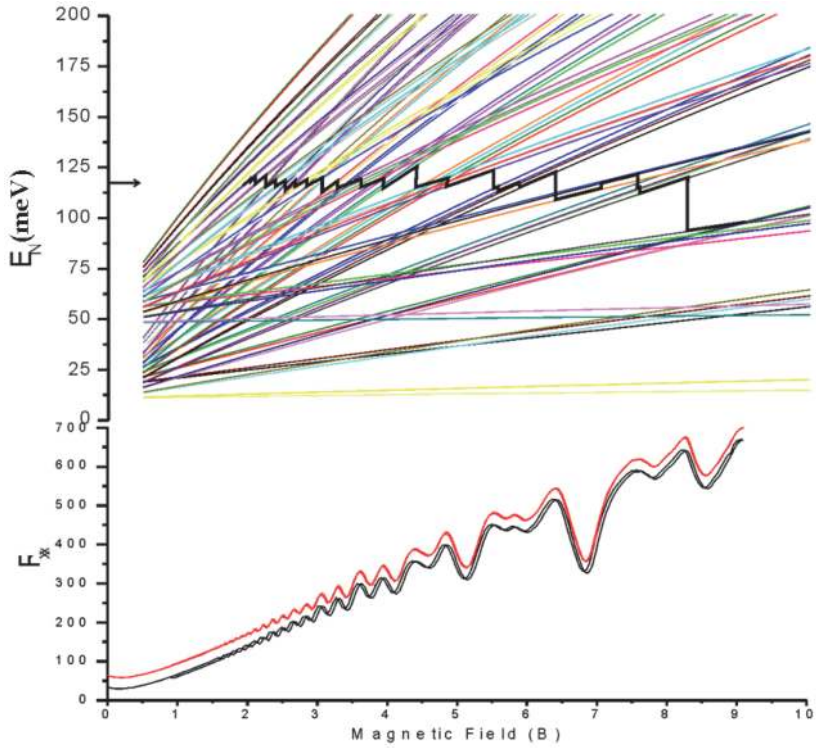

Figure 14.
Interpretation of Rxy (B) curve for DQW 2506 [15] .

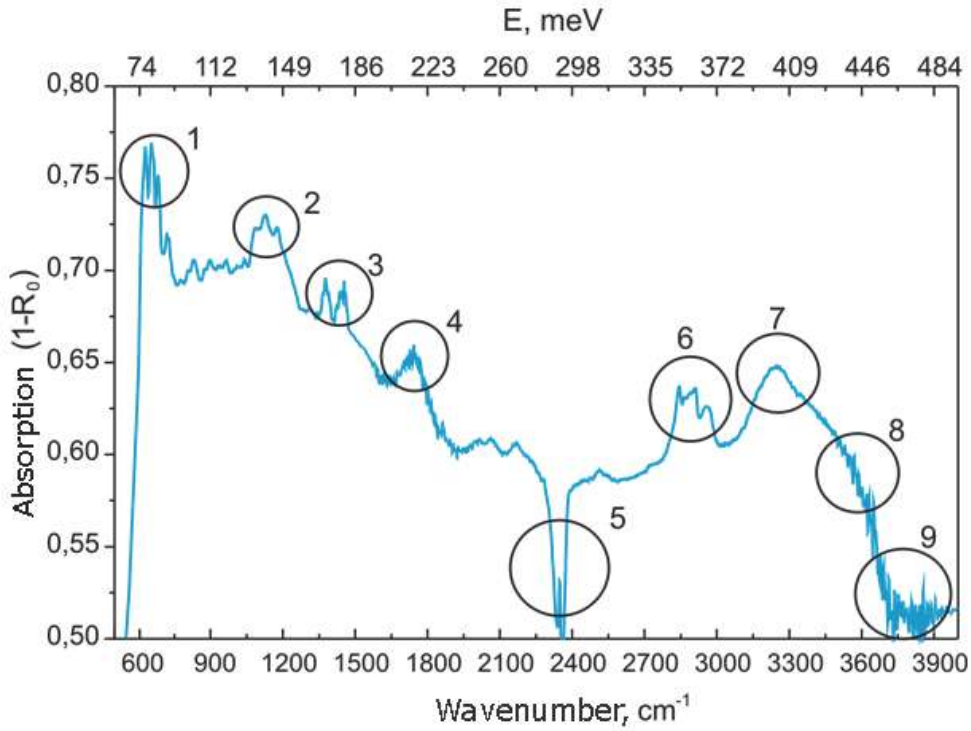

Figure 15.
Optical absorption curve obtained by averaging the optical reflection $\mathbf{R_o}$ *when scanning the sample surface 2506. The recorded absorption bands are renumbered (the double minimum 5 is due to the strong absorption of* CO_2 *in the atmosphere) [16].*

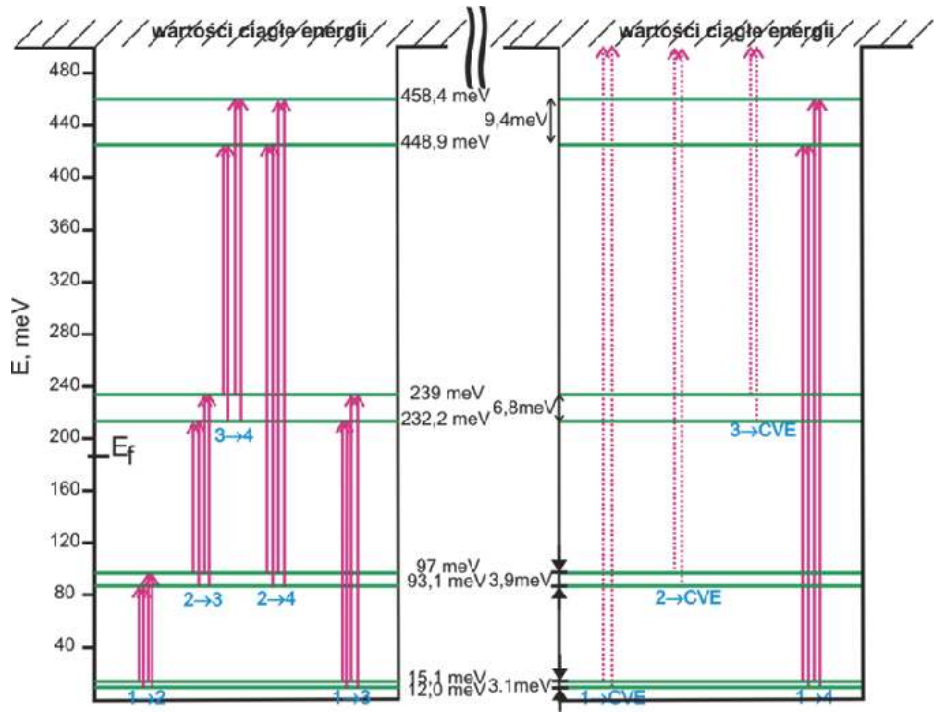

Figure 16.
The electron states in the DQW and optical transitions responsible for absorption bands shown in ***Figure 15****: 1 → 2 – band 1; 2 → 3 – band 2; 1 → 3 – band 3; 3 → 4 – band 4; 2 → 4 – band 6; 1 → 4 – band 7; 2 → CVE – band 8; 1 → CVE – band 9 [16].*

Supplying the infrared microscope with such a brilliant radiation source allowed for unique results [16]. For the first time, the energies of electron states were determined directly in DQW (see **Figures 15** and **16**) analogically as it was once done for the natural H_2 molecule [20]. From **Figure 16** it can be seen that the delta-SAS varies depending on the j number of the energy sub-band from 3.1 meV for $j = 1$ to 9.4 meV for $j = 4$.

3.9 Conclusion

The implementation of the quantum-mechanical problem of electron entrapment in a quantum well has been described. Various shapes of quantum wells—produced by advanced technologies as MBE and MOCVD, as well as based on different materials—are considered. Quantum wells based on GaAs/AlGaAs heterojunctions are especially important for the production of the semiconductor lasers, while the ones based on InGaAs/InAlAs heterojunctions are for the production of the HEMT transistors. Thanks to special engineering, it has been possible to make a *real rectangular potential of QW described by quantum-mechanical theory*.

Research into *double quantum wells* is a significant cognitive interest as an analogue of a two-atom hydrogen molecule in solid-state physics where essential role plays such quantum-mechanical phenomenon as *exchange interaction*. It can be predicted that their applications in electronics will also not make us wait long.

Author details

Eugen M. Sheregii
University of Rzeszow, Rzeszow, Poland

*Address all correspondence to: sheregii@ur.edu.pl

IntechOpen

© 2020 The Author(s). Licensee IntechOpen. This chapter is distributed under the terms of the Creative Commons Attribution License (http://creativecommons.org/licenses/by/3.0), which permits unrestricted use, distribution, and reproduction in any medium, provided the original work is properly cited. CC BY

References

[1] Herman MA, Richter W, Sitter H. Liquid phase epitaxy. In: Epitaxy. Springer Series in Materials Science. Vol. 62. Berlin, Heidelberg: Springer; 2004

[2] Alferov ZI, Andreev VM, Korol'kov VI, Portnoy EL, Yakovenko AA. AlAs-GaAs Heterojunction Injection Lasers with a Low Room-temperature Threshold Soviet Physics Semiconductors. 1969;**3**:460

[3] Alferov ZI. Nobel lecture: The double hetero-structure concept and its applications in physics, electronics, and technology. Reviews of Modern Physics. 2001;**73**:767

[4] Zawadzki W, Pfeffer P. Average forces in bound and resonant quantum states. Physical Review B: Condensed Matter and Materials Physics. 2001;**64**: 235313

[5] Herman MA, Sitter H. Molecular beam epitaxy. In: Fundamentals and Current Status. Springer Series in Materials Science. Vol. 7. Heidelberg: Springer Verlag; 1996

[6] Arthur JR, LePore JJ. GaAs, GaP, and $GaAs_xP_{1-x}$ Epitaxial films grown by molecular beam deposition. Journal of Vacuum Science and Technology. 1969; **6**:545

[7] Sakaki H. Prospects of advanced quantum nano-structures and roles of molecular beam epitaxy. In: International Conference on Molecular Bean Epitaxy. 2002. p. 5. DOI: 10.1109/MBE

[8] Mimura T. The early history of the high electron mobility transistor (HEMT). IEEE Transactions on Microwave Theory and Techniques. 2002;**50**(3):780-782

[9] von Klitzing K, Dorda G, Pepper M. New method for high-accuracy determination of the fine-structure constant based on quantized hall resistance. Physical Review Letters. 1980;**45**:494

[10] Girvin SM. The Quantum Hall Effect: Novel Excitations and Broken Symmetries. New York: Springer-Verlag; 1999

[11] Weisbuch C, Vinter B. Quantum Semiconductor Structures. San Diego: Academic Press; 2007

[12] Tomaka G, Sheregii EM, Kąkol T, Strupiński W, Jasik A, Jakiela R. Charge carriers parameters in the conductive channels of HEMTs. Physica Status Solidi (A). 2003;**195**(127)

[13] Sheregii EM, Ploch D, Marchewka M, Tomaka G, Kolek A, Stadle A, et al. Parallel magneto-transport in multiple quantum well structures. Low Temperature Physics. 2004;**30**:1146

[14] Płoch D, Sheregii EM, Marchewka M, Woźny M, Tomaka G. Magnetophonon resonance in double quantum Wells. Physical Review B. 2009;**79**:195434

[15] Marchewka M, Sheregii EM, Tralle I, Ploch D, Tomaka G, Furdak M, et al. Magnetospectroscopy of double quantum wells. Physica E. 2008;**40**: 894-904

[16] Marchewka M, Sheregii EM, Tralle I, Marcelli A, Piccinini M, Cebulski J. Optically detected symmetric and ant-symmetric states in double quantum Wells at room temperature. Physical Review B. 2009; **80**:125316

[17] Zawadzki W. Theory of optical transitions in inversion layers of narrow-gap semiconductors. Journal of Physics C: Solid State Physics. 1983;**16**:229

[18] Boebinger GS, Jiang HW, Pfeiffer LN, West KW. Magnetic-field-driven destruction of quantum hall states in a double quantum well. Physical Review Letters. 1990;**64**:1793

[19] Huang D, Manasreh MO. Effects of the screened exchange interaction on the tunneling and Landau gaps in double quantum wells. Physical Review B. 1996;**54**:2044

[20] Woodgate GK. Elementary Atomic Structure. Oxford: Clarendon Press; 1980